Development 134, 1397-1406 (2007) doi:10.1242/dev.02822

Specification of cell fate along the proximal-distal axis in the developing chick limb bud

Kosei Sato[1], Yutaka Koizumi[1], Masanori Takahashi[2], Atsushi Kuroiwa[3] and Koji Tamura[1,*]

Pattern formation along the proximal-distal (PD) axis in the developing limb bud serves as a good model for learning how cell fate and regionalization of domains, which are essential processes in morphogenesis during development, are specified by positional information. In the present study, detailed fate maps for the limb bud of the chick embryo were constructed in order to gain insights into how cell fate for future structures along the PD axis is specified and subdivided. Our fate map revealed that there is a large overlap between the prospective autopod and zeugopod in the distal limb bud at an early stage (stage 19), whereas a limb bud at this stage has already regionalized the proximal compartments for the prospective stylopod and zeugopod. A clearer boundary of cell fate specifying the prospective autopod and zeugopod could be seen at stage 23, but cell mixing was still detectable inside the prospective autopod region at this stage. Detailed analysis of HOXA11 AND HOXA13 expression at single cell resolution suggested that the cell mixing is not due to separation of some different cell populations existing in a mosaic. Our findings suggest that a mixable unregionalized cell population is maintained in the distal area of the limb bud, while the proximal region starts to be regionalized at the early stage of limb development.

KEY WORDS: Limb bud, Axis formation, Cell fate, Boundary, Chick

INTRODUCTION

Pattern formation during development is a complicated process that includes cell proliferation, migration, death and differentiation and is sometimes accompanied by subdivision of an area into domains with different and characteristic features. There are two basic mechanisms for generating different domains. One in which a uniform area is divided into several domains with different features. A good example of this can be seen in the rostral-caudal axis formation of the primary body in *Drosophila*, which involves a concentration gradient of molecules to specify the subdivisions. A second mechanism can be seen in the rostral-caudal axis of the primary body in vertebrates and short germ-band insects, in which domains with different features are sequentially added to the existing domains; at the tip of extension there is an area containing proliferative and undifferentiated progenitor cells from which new domains are generated.

During limb morphogenesis in tetrapod development, structures along the proximal-distal (PD) axis are established as a series of cartilage elements with an appropriate number and distinct morphology, and pattern formation of the structures serves as a fascinating model system for studying the establishment of domains in a developmental field. In a limb, there is a single long cartilage in the most proximal region (stylopod) followed by two long cartilage elements (the zeugopod), and the most distal structures of the limb are carpals/tarsals and digits (the autopod). Many studies on chick embryos, including observation of cartilage formation (Hinchliffe, 1977), apical ectodermal ridge (AER) removal experiments (Saunders, 1948; Summerbell, 1974; Lewis, 1975; Summerbell, 1976) and X-ray irradiation experiments (Wolpert, 1969), have suggested that the structure generated from the distal limb bud changes from the proximal part to the distal part as development proceeds. AER removal experiments have demonstrated that zeugopod specification has already started by chick stage 18-19, followed by autopod specification at stage 22-23 (Saunders, 1948; Summerbell, 1974; Lewis, 1975; Summerbell, 1976). The 'progress zone (PZ)' model, a widely accepted model for PD patterning in the limb bud, proposed on the basis of results of AER removal experiments and other experiments (Wolpert, 1969; Wolpert et al., 1975; Summerbell and Lewis, 1975), suggests that limb mesenchymal cells sequentially form more distal domains as they change their positional value, a characteristic of cells that determines which cartilaginous elements the cells will form with respect to the PD axis. It is assumed that a clock-like mechanism recording the time that mesenchymal cells spend in the PZ controls the positional value of a cell along the PD axis, but the molecular nature of this model remains unsolved.

An alternative model for PD axis formation, the prespecification model, has also been proposed (Stocum, 1975; Dudley et al., 2002; Sun et al., 2002). This model, a sort of subdivision model, assumes that cells in the early limb bud are previously specified as a pre-pattern of three layers for each future structure of the stylopod, zeugopod and autopod. This model is based not on a clock-like mechanism but a mechanism by which cells are specified into all regions along the PD axis at an early stage; e.g. gradation of a molecule along the axis. Evolutionary morphology (Richardson et al., 2004) and the results of a study on Gli3 and plzf functions in PD patterning (Barna et al., 2005) suggested that the distal and proximal structures of a limb are specified independently, supporting the prespecification model.

The exact mechanism of PD axis formation remains unclear because many results of experiments (Dudley et al., 2002; Sun et al., 2002; Tickle and Wolpert, 2002; Saunders, 2002; Wolpert, 2002; Richardson et al., 2004; Barna et al., 2005) can be mostly explained by both ideas. In order to further understand how limb mesenchymal cells acquire positional identity in terms of the PD axis, it is

[1]Department of Developmental Biology and Neurosciences, Graduate School of Life Sciences, Tohoku University, Aobayama, Aoba-ku, Sendai 980-8578, Japan. [2]Division of Developmental Neuroscience, CTAAR, Tohoku University School of Medicine, Seiryo-machi, Aoba-ku, Sendai 980-8575, Japan. [3]Division of Biological Science, Graduate School of Science, Nagoya University, Furo-cho, Chikusa-ku, Nagoya 464-8602, Japan.

*Author for correspondence (e-mail: tam@biology.tohoku.ac.jp)

Accepted 25 January 2007

important to elucidate their developmental destiny. Fate mapping, in which natural cell fate is solely traced as strictly as possible, is a simple but informative system for this purpose (Clarke and Tickle, 1999), and excellent fate maps of the chick limb bud (Saunders, 1948; Stark and Searls, 1973; Summerbell, 1976; Bowen et al., 1989; Vargesson et al., 1997) have resolved many issues of pattern formation in the developing limb. In the present study, we developed detailed and accurate fate maps of distal limb bud cells at early and late stages of limb development in order to address some fundamental questions about regionalization of cell fate along the PD axis. Our fate mapping of distal mesenchymal cells shows that there is no boundary of cell fate between the prospective autopod and zeugopod at an early stage (stage 19), whereas the regionalization for a more proximal region between the prospective stylopod and zeugopod can be seen at this early stage. The regionalization of the prospective zeugopod and autopod appears to be completed by stage 23. Detailed observations of HOXA11 and HOXA13 immunoreactivity show that the distal limb bud has no mosaic condition of expression of these proteins. Our findings demonstrate that only the distal limb bud is maintained in a mixable unregionalized condition and that each limb structure is likely to be regionalized in the proximal-to-distal direction.

MATERIALS AND METHODS

DiI and DiO administration and method for tracing cell fate

White Leghorn chicken eggs were incubated at 38°C and staged according to Hamburger and Hamilton (Hamburger and Hamilton, 1951). Limb bud cells were labeled with the lipophilic dye DiI (1,1-dioctadecyl-3,3,3′,3′-tetramethyl indocarbocyanine perchlorate; Molecular Probes) and DiO (3,3′-dioctadecyloxacarbocyanine, perchlorate; Molecular Probes) prepared after the method of Li and Muneoka (Li and Muneoka, 1999). To standardize the size of samples, embryos with limb buds of similar sizes were selected from embryos of the same stage. Areas used for mapping were about 1200 μm along the anterior-posterior axis and about 250 μm along the proximal-distal axis of stage 19 limb buds, and about 1200 μm along the anterior-posterior axis and 1200 μm along the proximal-distal axis of stage 23 limb buds. Dye administration by pressure of expiration was performed using a pulled micropipette with a tip opening of approximately 6-15 μm in diameter. In order to determine the position and area injected with dye, labeled limb buds were observed and photographed under a fluorescence microscope immediately after dye administration, and then the size of the dye spot and the distance from the AER were calculated with the aid of a micrometer (see Fig. 1A,D,G,J). For accurate evaluation of the injection point at stage 23, the distal limb bud was excised out on a dish after labeling, observed under a microscope, and then put back on the amputated plane of the same limb bud with a tungsten wire. The prospective middle finger region [estimated after Vargesson et al. (Vargesson et al., 1997)] was targeted for the injection point. At 2 days after the above process, operated limb buds were photographed and stained for cartilage. Whole-mount in situ hybridization for proteoglycan-H (for samples labeled at stage 19), a good marker for cartilage condensation (Mallein-Gerin et al., 1988), and Alcian Blue staining (for samples labeled at stage 23) were used for cartilage pattern observation. Whole-mount in situ hybridization was performed as described by Yonei et al. (Yonei et al., 1995), and digoxigenin-labeled RNA probes were prepared according to the method of Yokouchi et al. (Yokouchi et al., 1991). For Alcian Blue staining, embryos were fixed overnight in 10% formalin in Tyrodes solution, stained with 0.1% Alcian Blue in 70% ethanol with 0.1 M HCl at 37°C overnight, dehydrated, and cleared in methyl salicylate. In some experiments, sections were cut with a cryostat following a protocol described by Li and Muneoka (Li and Muneoka, 1999).

Real-time RT-PCR and immunohistochemistry for HOXA11 and HOXA13

RNA was isolated from the distal limb bud using an RNeasy total RNA isolation kit (Qiagen). Quantitative analysis was performed using a Lightcycler Quick System 350S (Roche) for 40 cycles of a two-step PCR amplification (95°C for 5 seconds and 60°C for 20 seconds). The amounts of amplified PCR products were monitored in each cycle during PCR with SYBR Green I (Roche) added as a fluorescent material. *HOXA11*- and *HOXA13*-specific primers, yielding product sizes as indicated were *HOXA11* (169 bp) [forward primer, 5′-ATCTTCCGGCAACAATGAGG-3′ (20mer); reverse primer, 5′-CAGATTGAGCATTCGGGAGA-3′ (20mer)], *HOXA13* (173bp) [forward primer, 5′-GTGGAACGGGCAAGTGTACT-3′ (20mer); reverse primer, 5′-GCGTATTCCCTTTCGAGTTC-3′], β-actin (165bp) [forward primer, 5′-TCTGACTGACCGCGTTACTC-3′ (20mer); reverse primer, 5′-CCATCACACCCTGATGTCTG-3′ (20mer)]. These primer sets were based on the chick *HOXA11* mRNA sequence (GenBank NM_204619), *HOXA13* mRNA sequence (GenBank AY030050), and β-actin mRNA sequence (GenBank L08165), respectively. Relative standard curves for *HOXA11* and *HOXA13* were constructed using fivefold serial dilutions of cDNA derived from distal limb bud at stage 24 and 26, respectively. Data were based on a threshold cycle (Ct) in which the signal was higher than that of the background. For quantitative comparison of gene expression, the amount of *HOXA11* and *HOXA13* expression was standardized with that of β-actin. The relative amount of *HOXA11* and *HOXA13* expression of cDNA derived from the chick limb region at stage 20 was taken as 1.0. Gene expression levels in samples were compared using Student's matched-pair *t*-test.

Immunohistochemical staining using a specific antibody against chick HOXA11 and HOXA13 was performed as described previously (Yamamoto et al., 1998; Hashimoto et al., 1999; Suzuki and Kuroiwa, 2002).

RESULTS

Mapping fate along the PD axis of distal mesenchymal cells at chick stage 19

A previous cell-labeling experiment (Dudley et al., 2002) showed that three areas at different locations along the PD axis of chick stage 19 limb buds contribute to the stylopod, zeugopod and autopod, respectively, suggesting that segments for each future structure have already been specified as distinct domains at this stage. To obtain further information about the boundaries between these domains along the PD axis, we began by constructing a detailed fate map of a stage 19 limb bud to examine prospective fates of limb mesenchymal cells along the PD axis.

In order to examine the prospective fate of the distal limb bud, some distal mesenchymal cells were labeled with DiI and observed 2 days later. Before constructing fate maps, we evaluated our procedure for fate mapping from several viewpoints. First, we confirmed that there was no leaky diffusion of DiI during experiments. When the operated embryo was fixed after DiI administration and left on a dish for 2 days at 4°C, there was no diffusion of DiI fluorescence in the embryo within 2 days (see Fig. S1A-C in the supplementary material). Taken together with the fact that DiI and DiO have been widely used for studying cell fate (Clarke and Tickle, 1999; Kimura et al., 2006), it is certain that fluorescence for DiI and DiO in living embryos at 2 days after labeling does not include leaky diffusion, indicating that the signal represents only the distribution of cells labeled 2 days ago and their progeny. We also evaluated whether the dorsal view of limb buds indicates the correct position of labeled cells in the cartilage-forming core region. DiI fluorescence was detected in a straight belt along the dorsal-ventral axis in longitudinal sections (see Fig. S1D-H in the supplementary material), revealing that the fluorescence observed from the dorsal side of the limb bud corresponds to that in the core region. A condensed cell population forming cartilage was sometimes labeled in the core region, confirming that our labeling method gives rise to no bias toward cell type. In addition, it is likely that the central region (cartilage-forming area) and peripheral region (non-cartilaginous area) of the limb bud have similar prospective fates along the PD axis.

When the area 0-40 μm from the AER was labeled (Fig. 1A), the DiI-labeled area was found in the autopod 2 days later (Fig. 1B,C). The area 0-60 μm from the point in the AER labeled with DiI (Fig. 1D) was distributed to the distal part of the zeugopod and the entire autopod (Fig. 1E,F). The area 120-180 μm from the AER (Fig. 1G) was found in a region from the proximal end of the zeugopod to a proximal point in the autopod (Fig. 1H,I). The area 180-230 μm from the AER (Fig. 1J) was found in the inside of the zeugopod (Fig. 1K,L). These results, particularly the results shown in Fig. 1D-F, suggested that the area 0-60 μm from the AER contains cells that can contribute to the formation of both the autopod and zeugopod (Fig. 1E,F). To further examine whether the distal area forms the zeugopod as well as the autopod, double labeling was performed; an area 50 μm from the AER was first labeled with DiI (Fig. 2A) and the proximal edge of the DiI distribution was labeled with DiO 2 days later (Fig. 2B-D). Another 2 days later, DiO-labeled cells were clearly observed in a distal portion of the zeugopod (Fig. 2E,F), indicating that the proximal end of the first-labeled area contributed to the formation of the zeugopod.

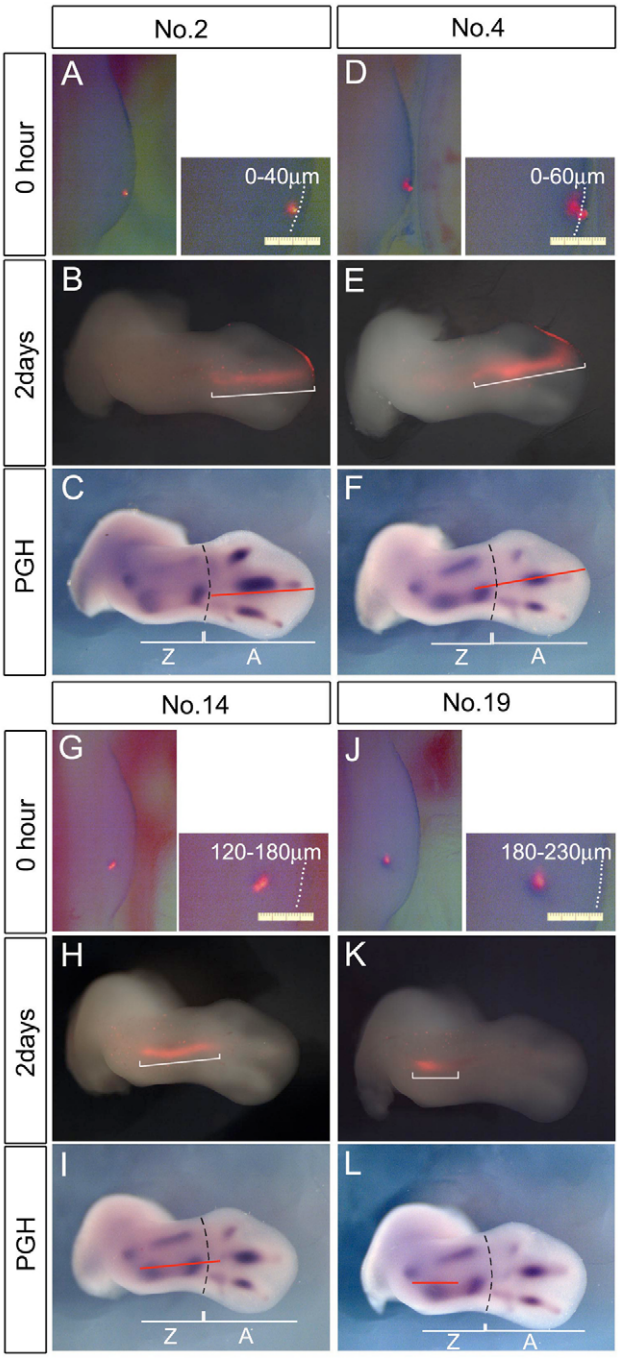

Fig. 1. Examples of DiI labeling of stage 19 limb buds. Four independent specimens, sample numbers 2 (**A-C**), 4 (**D-F**), 14 (**G-I**) and 19 (**J-L**), are shown. The top row (A,D,G,J) in each sample shows the limb bud immediately after labeling. The injected point is magnified in the right panel. Scale bar: 200 μm. The white dotted line shows the base of the AER. (B,E,H,K) The same limb bud as that shown in the top row after 2 days. (C,F,I,L) Cartilage pattern [visualized by proteoglycan-H (PGH) expression] of the same limb bud as that shown in the images in the middle row. Red lines indicate fluorescence-positive regions in B,E,H,K (indicated by brackets). Broken lines divide the zeugopod (Z) and autopod (A), estimated by PGH expression.

Fig. 3 shows a diagram of a fate map of limb mesenchymal cells at stage 19, constructed from 27 independent samples of fate-tracing experiments, typical examples of which are shown in Fig. 1. Bars assigned to the stylopod (Fig. 3B) originated from seven samples as shown in Fig. 3A [from sample 19 (180-230 μm from the AER) to sample 27 (270-320 μm from the AER)]. The bar of sample 17 (160-210 μm from the AER) and bars of samples labeled in a more distal region are not assigned to the stylopod, and it could therefore be interpreted that the area 230 μm, and more, from the AER at stage 19 is the prospective stylopod region (summarized also in Fig. 7A). On the other hand, bars assigned to the zeugopod (Fig. 3B) originated from 22 samples as shown in Fig. 3A [from sample 3 (0-50 μm from the AER) to sample 24 (220-270 μm from the AER)]. The bar of sample 2 (0-40 μm from the AER) and that of sample 25 (240-280 μm from the AER) are not assigned to the zeugopod, and it could therefore be interpreted that the area 50-240 μm from the AER at stage 19 is the prospective zeugopod region. Bars assigned to the autopod (Fig. 3B) originated from 17 distal samples in Fig. 3A [from sample 1 (0-30 μm from the AER) to sample 17 (160-210 μm from the AER)]. The bar of sample 18 (180-210 μm from the AER) and bars of samples labeled at a more proximal region are not assigned to the autopod. Therefore, it could be interpreted that at least the region 160 μm from the AER of the chick stage 19 limb bud is the prospective autopod region (summarized in Fig. 7A).

Our fate map demonstrates that prospective stylopod and zeugopod regions are located in relatively distinct domains in a stage 19 limb bud, as suggested by a previous study (Dudley et al., 2002). In contrast to this, prospective autopod and zeugopod regions tend to overlap each other at 50-160 μm from the AER, and these two regions seem not to have an obvious boundary of cell fate (see also Fig. 7A).

To obtain direct evidence supporting this idea, two distant regions in a stage 19 limb bud were simultaneously labeled with DiI and DiO. When two proximal regions were labeled with DiI (220-240 μm from the AER; Fig. 4A) and DiO (250-330 μm from the AER; Fig. 4B), DiI- and DiO-labeled cells contributed to the zeugopod and stylopod, respectively, showing that there are distinct domains for prospective zeugopod and stylopod regions at stage 19 (Fig. 4C-F). When two distal regions were labeled with DiI (0-70 μm from the AER; Fig. 4G) and DiO (120-170 μm from the AER; Fig. 4H), DiI- and DiO-labeled cells were mixed at the cartilage zeugopod-autopod boundary (Fig. 4I-L). Similar results were obtained (Fig. 4M-T) when an area 10-50 μm from the AER was labeled with DiI (Fig. 4M) and a more proximal area (150-210 μm) was labeled with DiO (Fig. 4N). Detailed observation of red and green fluorescence in

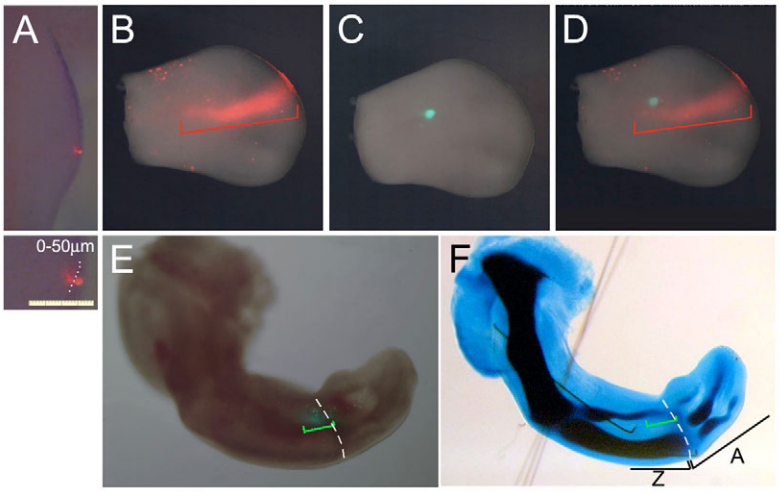

Fig. 2. Two-step labeling of a **stage 19 limb bud.** (**A-C**) The distal limb bud (0-50 μm from the AER) was first labeled with DiI (A; an enlargement of the area is shown below, scale bar: 200 μm). After 2 days, the distal tip of the DiI-labeled limb bud was cut out and placed on a dish, and the proximal end of the DiI-labeled region (indicated by bracket in B) was then labeled with DiO (C). (**D**) Merged image of B and C, showing that the second labeling of DiO successfully marks the end of the first labeling of DiI. (**E**,**F**) The same sample as that in B-D was observed for DiO signal (E) and cartilage (Alcian Blue staining, F). The broken line in E divides the zeugopod (Z) and autopod (A) estimated from the Alcian Blue staining.

sections revealed clear overlapping of DiI and DiO at the same level (Fig. 4O-T). These results strongly support the idea that the boundary of prospective zeugopod and autopod regions is indefinite at stage 19 in the chick.

Fate of distal mesenchymal cells along the PD axis at chick stage 23

Having established a map, showing overlapping cell fate of the prospective zugopod and autopod regions at stage 19, we next framed a fate map at stage 23, focusing on these two regions. Two areas (0-60 μm and 140-200 μm from the AER) were labeled with DiI and DiO, respectively (Fig. 5A,B). After excising the labeled distal tip of the stage 23 limb bud on a dish, the labeled area was measured under a microscope and the tip was pinned back on the amputated plane. Two days after the labeling, the DiI-labeled area was found in the metacarpal and digit regions, and the DiO-labeled area was found in the carpal and metacarpal regions (Fig. 5C-E). Areas at 0-90 μm (DiI) and 230-280 μm (DiO) from the AER (Fig. 5F,G) were found in the metacarpal-digit and carpal regions, respectively (Fig. 5H-J). Areas at 300-

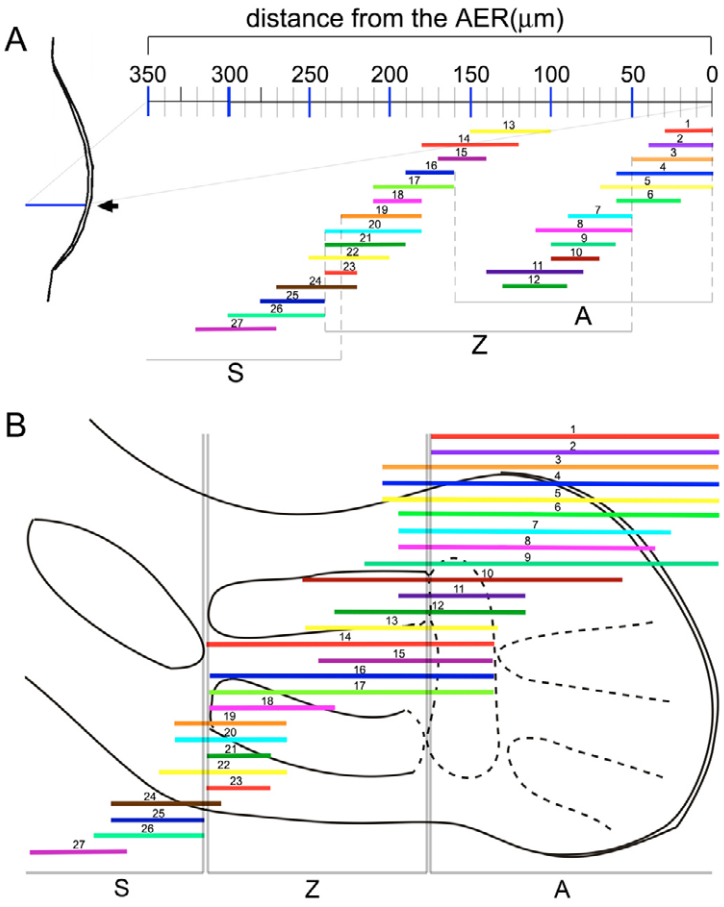

Fig. 3. Diagrams of fate maps based on results of 27 independent labeling experiments at stage 19. Sample number is shown over each bar. (**A**) Representative stage 19 wing bud, showing positions at which DiI was injected. Graduations on the scale bar indicate the distance from the AER. Each colored bar under the scale shows the width of area labeled with DiI at 0 hours in each experiment. (**B**) Contribution of labeled cells 2 days later. Colors and numbers correspond in A and B. Note that the position of each bar on the anterior (top)-posterior (bottom) axis does not indicate the labeled position along the axis but that DiI was always injected in the prospective digit 3 region indicated by an arrow in A. S, stylopod; Z, zeugopod; A, autopod.

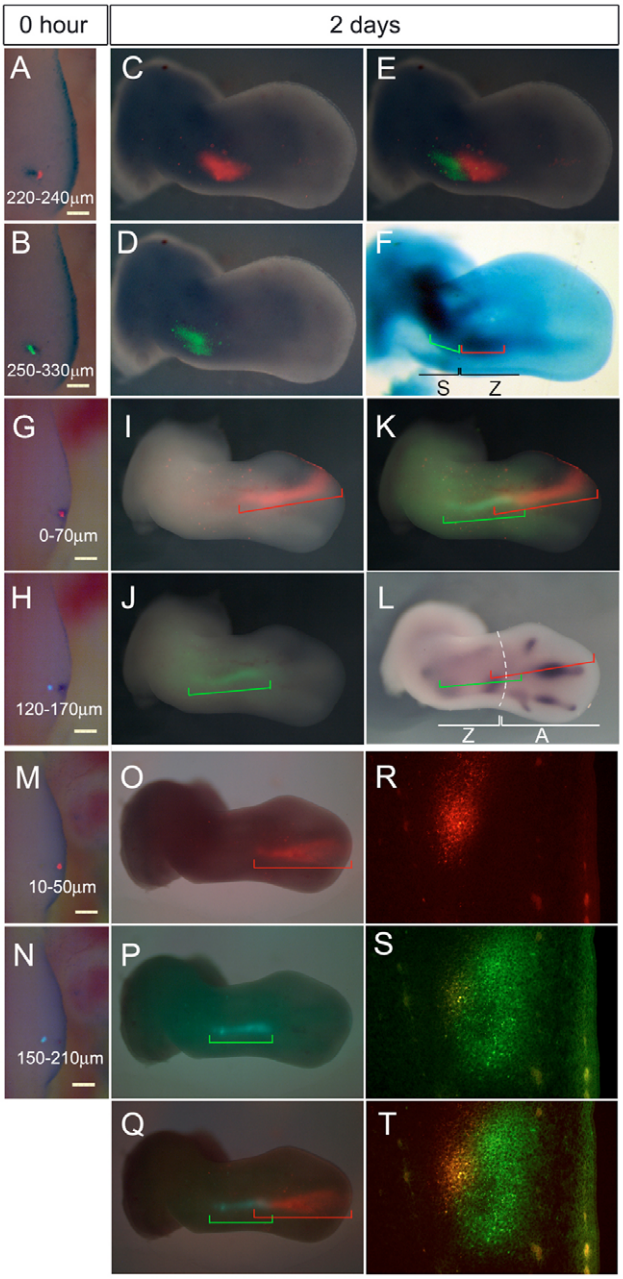

Fig. 4. Double labeling with DiI and DiO in the same limb bud at stage 19. (**A**,**B**) Proximal two regions (A; 220-240 μm, B; 250-330 μm from the AER) were simultaneously labeled with DiI (red) and DiO (green). (**C-F**) Contribution of labeled cells 2 days later. The two signals are observed only within the zeugopod (Z) and stylopod (S), respectively (C,D), with a small overlap (E,F) (Alcian Blue staining, F). (**G**,**H**) Distal two regions (G; 0-70 μm, H; 120-170 μm from the AER) of the same limb bud were simultaneously labeled with DiI and DiO. (**I-L**) Contribution of labeled cells 2 days later. Note that overlapping of DiI (I) and DiO (J) signals (indicated in yellow in K) crosses the zeugopod-autopod boundary evident in the cartilage pattern (L). (**M**,**N**) Similar labeling experiment as that in G,H was performed. Labeled two regions are 10-50 μm (M) and 150-210 μm (N) from the AER of the same limb bud. (**O-Q**) Whole-mount observation of fluorescent signal in the same limb bud 2 days later than that shown in M,N. Fluorescence for DiI (O) and that for DiO (P) overlap. (**R-T**) Higher magnification of cross-sections of the overlapping area (detected in yellow and indicated by an arrow in Q) was sectioned. Both DiI (R) and DiO (S) are detected in the region of overlap (T). Scale bars: 100 μm.

340 μm (DiI) and 400-460 μm (DiO) from the AER (Fig. 5K,L) contributed to the formation of carpal and zeugopod regions, respectively (Fig. 5M-O).

The results of 27 experiments on stage 23 chick embryos are summarized in Fig. 5P,Q. Since bars assigned to the autopod are derived from sample 1 (0-50 μm from the AER) to sample 21 (390-450 μm) and since sample 22 (400-460 μm) does not contribute to the formation of the autopod, the distal area, up to 390 μm from the AER is the prospective autopod region. However, bars assigned to the zeugopod are from samples 18 (300-350 μm) to 27 (550-610 μm), indicating that the prospective zeugopod is in the area 350 μm and more proximally, from the AER. Overlap of the prospective zeugopod and autopod regions at chick stage 23 is expected to be within only 40 μm (350-390 μm), and it is therefore thought that prospective zeugopod and autopod regions are more regionalized by stage 23. Since some bars (sample 2 to sample 10) are assigned to both the phalanx and metacarpal regions with considerable overlap, it is thought that the area within 150 μm of the distal limb bud at stage 23 is not fully regionalized. Therefore, regionalization inside the autopod seems more incomplete than that of the zeugopod and autopod at this stage (see also Fig. 7B).

HOXA11 and HOXA13 expression in distal mesenchymal cells of the limb bud at various stages

Our fate mapping, demonstrating that mixed cell fate (zeugopod and autopod at stage 19, and metacarpal and phalanx at stage 23) was maintained in the distal limb bud, suggests that the distal region contains some different cell populations in mosaic. To investigate this possibility, we examined protein expression in the distal limb bud at the cellular level. We chose two molecules, HOXA11 and HOXA13, as markers for molecular properties in the distal region. Expression patterns of these genes are known to change in the region (Yokouchi et al., 1991; Nelson et al., 1996), and moreover, our quantitative real-time RT-PCR analysis revealed that these two marker genes also have different amounts of transcripts in distal limb buds (see Fig. S2 in the supplementary material).

To determine whether the cells of the distal limb bud have different combinations of these markers, we investigated localization of HOXA11 and HOXA13 proteins recognized by specific antibodies for each protein (Yamamoto et al., 1998; Hashimoto et al., 1999; Suzuki and Kuroiwa, 2002). At stage 20, neither HOXA11 nor HOXA13 immunoreactivity was detected in the distal mesenchyme (Fig. 6A,Fa-Fc). At stage 21, HOXA11 immunoreactivity was detected in the distal mesenchyme in a graded manner along the PD axis (high in the distal and low in the proximal domain; Fig. 6B,Ga-Gc). At stage 22, HOXA13-positive cells were first detected in the distal-peripheral mesenchyme in a layer about five cells thick within the HOXA11-positive domain (Fig. 6C,Ha-Hc). At stage 24, HOXA11-HOXA13-double-positive mesenchymal cells had expanded in the core of the distal limb bud (Fig. 6Ia-Ic). At stage 26, the expression domain of HOXA13 had expanded to a more proximal region, and almost all of the immunoreactivity for HOXA11 protein had disappeared in the HOXA13-positive domain (Fig. 6E,Ja-Jc). As a result, no mosaic localization of these proteins was observed at any stage examined. Confocal microscopy at single cell resolution further supported this (Fig. 6K-N). At stage 24, both HOXA11 and HOXA13 proteins were expressed in all of the nuclei in the distal limb bud. Both signals were observed as particles patchily distributed in

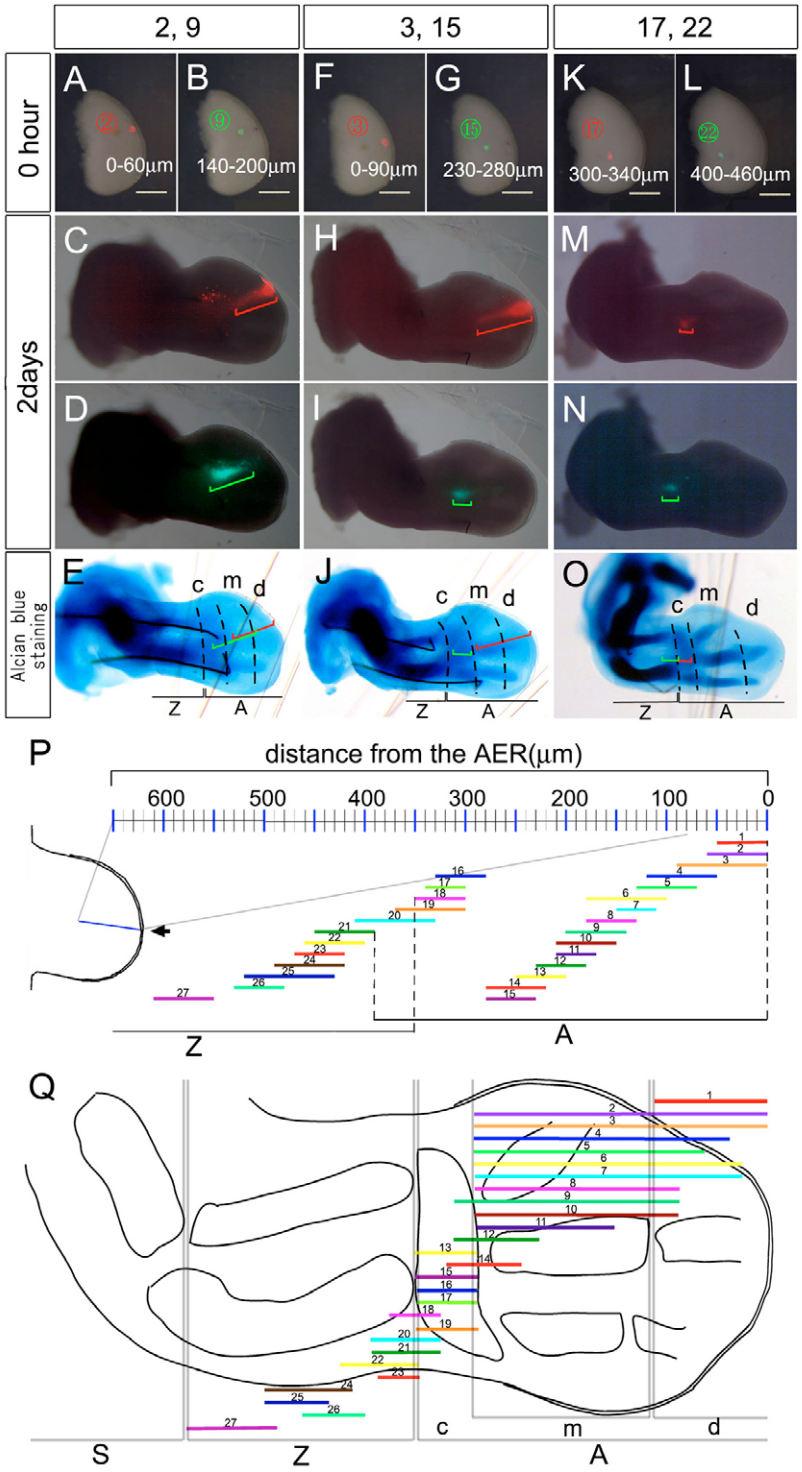

Fig. 5. Fate mapping of a stage 23 limb bud. (**A-O**) Three independent specimens, sample numbers 2 and 9 (A-E), 3 and 15 (F-J), and 17 and 22 (K-O), are shown. (A,B,F,G,K,L) The limb buds immediately after labeling. In each sample, both DiI (A,F,K) and DiO (B,G,L) were injected into different levels (as indicated) at the same time. (C,D,H,I,M,N) The contribution of labeled cells after 2 days in the same limb bud as that shown in the top row. The fluorescence-positive region is indicated by brackets. (E,J,O) The cartilage pattern (visualized by Alcian Blue staining) of the same limb bud as that shown in the middle rows. Dashed lines divide the skeletal pattern into a series of proximal-distal parts. Scale bar: 300 μm. (**P**,**Q**) Diagrams showing a fate map based on results of 27 labeling experiments at stage 23. Graduations on the scale bar in P indicate the distance from the AER. Colored bars under the scale show the area labeled with DiI or DiO in each sample. Q shows the contribution of labeled cells in the middle finger region 2 days after labeling. S, stylopod; Z, zeugopod; A, autopod; c, carpal; m, metacarpal; d, digit.

nuclei, and these signals were sometimes colocalize, and all mesenchymal cells we observed were HOXA11-positive and HOXA13-positive in the distal region of a stage 24 limb bud (Fig. 6N).

Although these results suggest that the limb bud has a homogeneous cell population within a certain width of the distal region, they do not necessarily mean that the width of the homogeneous distal region is constant. Rather, the HOXA13-positive domain became wider as limb bud development proceeded (Fig. 6A-E). Interestingly, the width of the HOXA13-positive domain at stage 23 (increased to around 234 μm; Fig. 6D) was smaller than that of the prospective autopod region shown by our fate map (around 380 μm; Fig. 5P).

DISCUSSION

Regionalization of prospective stylopod, zeugopod and autopod regions along the PD axis

The fate map of a stage 19 limb bud constructed in this study demonstrates that the prospective stylopod covers the most proximal area, 230 μm and more from the AER and that the prospective

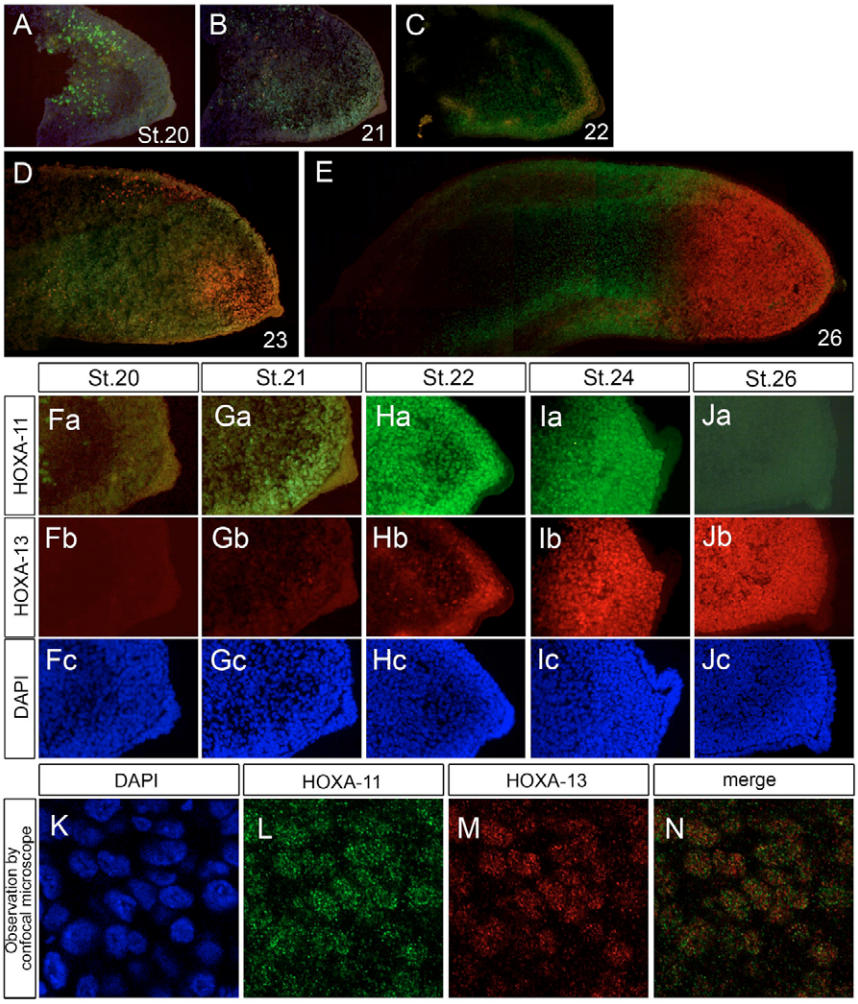

Fig. 6. Non-mosaic expression of HOXA11 and HOXA13 in the distal mesenchymal cells. (**A-E**) Immunohistochemical double-staining for HOXA11 (green) and HOXA13 (red) at stage 20 (A), stage 21 (B), stage 22 (C), stage 23 (D) and stage 26 (E). All images are longitudinal sections of the distal limb bud at prospective third finger position, oriented with dorsal to the top and distal to the right. All images are at the same magnification. (**Fa-Jc**) Higher magnification of the distal limb buds. HOXA11 (Fa,Ga,Ha,Ia,Ja) and HOXA13 (Fb,Gb,Hb,Ib,Jb) do not show any mosaic expression at any of the stages we examined. This was confirmed by confocal microscopic observation at stage 24 (**K-N**). Both proteins are localized in all of the nuclei. Note that signals are detectable as particles, which appear yellow in the merged figure (N).

zeugopod ranges from 50 to 240 μm in the subdistal region (Fig. 3A, Fig. 7A), suggesting that prospective stylopod and zeugopod regions are located in distinct domains with small overlap at this early stage. These findings are consistent with the results of a previous study (Dudley et al., 2002) showing that cells marked 100-200 μm and 200-300 μm from the AER ended up exclusively in the zeugopod and stylopod, respectively. In contrast to this agreement, our fate map suggests that there is still a large overlap between the prospective zeugopod and autopod regions at this stage [the wrist (carpal) region is defined as a part of the autopod in this study]. The most distal region, at 0-160 μm was classified as the prospective autopod, whereas the prospective zeugopod ranged from 50 to 240 μm (Fig. 3A, Fig. 7A). The extent of overlap (around 110 μm) corresponds to 69% of the prospective autopod region (around 160 μm) and 58% of the prospective zeugopod region (around 190 μm). Many spots labeled at 50-160 μm from the AER were found in both the zeugopod and autopod, and, moreover, two distant spots were merged with each other. We propose that distal mesenchymal cells of a stage 19 limb bud intermingle with each other along the PD axis and that there is no boundary of cell fate between the prospective autopod and zeugopod at this stage. Although this idea appears to oppose the conclusion in the previous report (Dudley et al., 2002) that future structures of the stylopod, zeugopod and autopod are specified as a pre-pattern of three regions at this early stage, the actual data do not contradict each other but can be reconciled. We showed that there were some points that only contributed to the stylopod, zeugopod or autopod [see sample numbers 25, 26, 27 (stylopod), 18, 21, 23 (zeugopod), 1, 2 (autopod) in Fig. 3] as was reported by Dudley et al. (Dudley et al., 2002). Our detailed labeling revealed the overlap between autopod and zeugopod, which was missed by Dudley et al. (Dudley et al., 2002) because they failed to examine intermediate injection levels. Our results, showing that the proximal part of a stage 19 limb bud is regionalized but that the distal bud is not, suggest that the early stage limb bud has some different properties along the PD axis. Since all limb mesechymal cells at this stage are thought to be within range of the FGF signaling from the AER [as evaluated by expression of FGF-responding genes (Minowada et al., 1999; Corson et al., 2003; Eblaghie et al., 2003; Kawakami et al., 2003)], it is interesting that the proximal and distal cells behave differently under the FGF signaling. In this sense, we suggest that the early limb buds already have a partial regionalization along the PD axis.

At stage 23, the extent of the overlapping region for the autopod and zeugopod decreased to 40 μm, about 10% of the prospective autopod region (Fig. 7B), suggesting that regionalization of the prospective zeugopod and autopod is almost completed by stage 23. In contrast to this, the location of cells that contribute to the formation of more distal structures within the autopod, such as metacarpals and phalanx, overlapped even at this stage (Fig. 7B). Therefore, it is likely that the domains for the prospective structures along the PD axis are progressively regionalized in the proximal-to-distal direction.

How do mesenchymal cells acquire positional identity along the PD axis?

From our fate maps, we found considerable cell mixing in the distal limb bud. At stage 19, the main region where cell mixing occurs is located around 160 μm from the AER (Fig. 7A). For example in Fig. 3A, the bar of sample 1 (0-30 μm from the AER) and the bar of sample 17 (160-210 μm from the AER), which had been located distant from each other at stage 19, overlapped at the wrist level after 2 days, indicating that these two distant areas at stage 19 include cells that move in this area and can be distributed at the same level. At stage 23, such a region with cells of mixed origins can also be observed in a similar range (0-150 μm; Fig. 7B). This situation, wherein cells may change their proximal-distal location, seems to be a characteristic of the distal limb bud because at both stage 19 and stage 23 proximal mesenchymal cells showed much smaller dispersion and little mixing along the PD axis (indicated by short bars in the proximal region in Fig. 3 and Fig. 5). At stage 19, prospective stylopod and zeugopod domains only have small overlap outside the distal region 160 μm from the AER (Fig. 7A). Similarly, at stage 23, the prospective zeugopod and autopod are regionalized in the proximal (more than 150 μm from the AER) limb bud (Fig. 7B). These results suggest that regionalization and compartmentalization along the PD axis are organized in the proximal limb bud. Our detailed observation of HOXA11 and HOXA13 distribution at the single cell resolution (Fig. 6), showing that individual cells go through transitions of expression, does not support the possibility that the distal region, in which mixed cell fate is maintained, contains some different cell populations in mosaic. It is unlikely that cell mixing in the distal limb bud occurs between cells that have different HOXA expression.

Our fate maps also suggested that a cell population at later stages contributes to a more restricted small region along the PD axis. For example, at stage 19, a mixed cell population (in a distal area about 150 μm from the AER) produces both the distal portion of the zeugopod and the entire autopod (indicated by a red line in Fig. 7C). By contrast, at a later stage (stage 23), a cell population within the same region of the distal limb bud more restrictedly contributes only to the formation of the autopod (a part of the metacarpal region and more distal region, indicated by a red line in Fig. 7D). It seems that mesenchymal cells that stay in the distal area (within 150 μm from the AER) during stages 19-23 contribute to the formation of the distal autopod at stage 23 and that mesenchymal cells that cannot remain in the distal area contribute to the zeugopod and proximal part of the autopod (carpal region). Although it remains unclear what determines whether mesenchymal cells remain in the distal area or to move out into the proximal area, it is possible that prospective fate is determined according to the final position of the cells under a mixable condition in the distal limb bud.

Although it seems that the mixable situation of the distal limb bud is reminiscent of the 'progress zone' in the progress zone model, our diagrams suggested that the distal fate does not represent an equivalency of positional identity in a certain distal region, an implicit trait of the 'progress zone'. The diagrams indicate that there are some regional differences in terms of prospective fate even within the distal 150 μm area. At stage 19, for example, we can see at least two distinct regions in the distal area that have different fates: the region 0-50 μm from the AER is an exclusive autopod-forming region, whereas the more proximal region (50-160 μm from the AER) contributes to the formation of both the autopod and zeugopod (see Fig. 7A). Also at stage 23, the distal domain can be separated

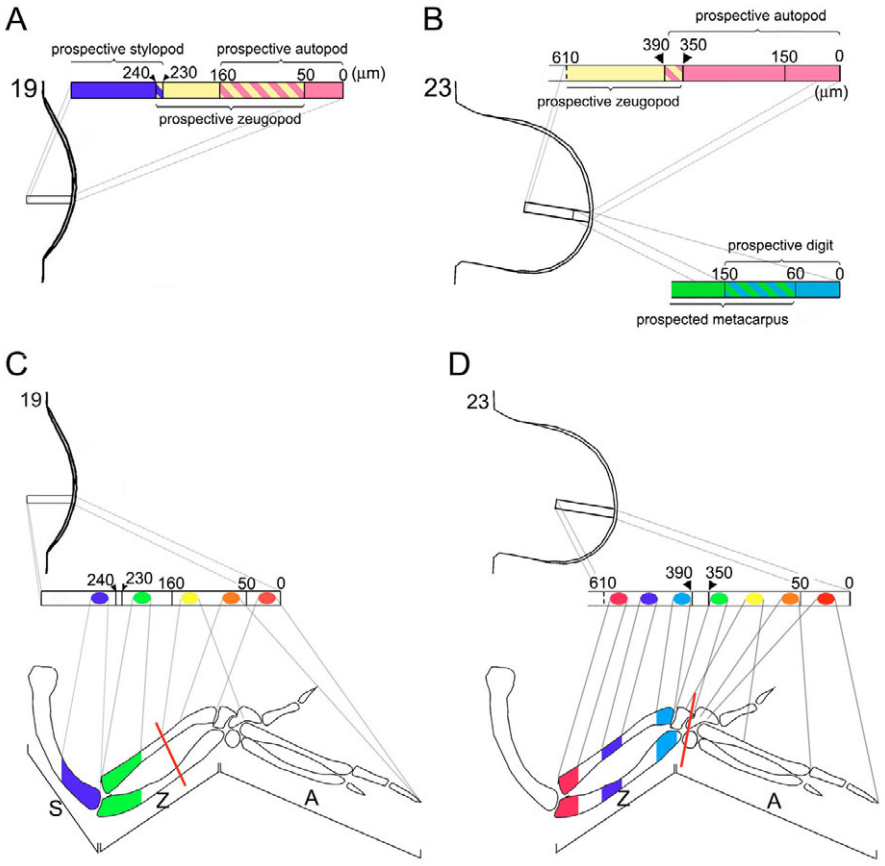

Fig. 7. Prospective fate of mesenchymal cells along the proximal-distal axis. (**A**,**B**) Diagram showing the prospective fate of different proximal-distal positions of the limb bud. (A) At stage 19, prospective zeugopod (yellow) and autopod (pink) regions have a large overlap (hatched) in the distal limb bud. In contrast to this, prospective stylopod (blue) and zeugopod regions are more regionalized in terms of developmental fate with a small overlap in the proximal limb bud. (B) At stage 23, the overlap between prospective zeugopod and autopod regions is reduced in the proximal limb bud. However, prospective metacarpus (green) and digit (light blue) regions still have a large overlap in the distal limb bud. (**C**,**D**) Diagram showing the contribution of mesenchymal cells to different proximal-distal positions of limb. At both stage 19 (C) and stage 23 (D), proximal mesenchymal cells show small dispersion and small degree of mixing along the PD axis. Meanwhile, distal mesenchymal cells are dispersed widely along the PD axis and show remarkable mixing. Red lines in C and D show the proximal end of the structure derived from the distal 150 μm region from the AER.

into two regions: future phalanx-forming region (distal 0-60 μm area) and more proximal region (60-150 μm area) (see Fig. 7B). Although it appears that the distal region contains mesenchymal cells that have equal developmental potential, the regionalization along the PD axis may emerge at the distal tip and gradually proceed to the proximal end, and in this sense, all cells at different positions along the PD axis may possess slightly different identities even in the distal domain.

HOXA11 and HOXA13 are accurate molecular markers for the PD axis in the limb, the final expression domains of which are exclusive to each other along the PD axis. Whereas they seems not themselves involved in specifying the limb segments (but rather for differentially controlling growth within distinct segments), HOXA11 and HOXA13 are the best markers we have for these limb segments. These molecules, however, do not always have the same expression in the limb bud but show drastic changes in expression spatially and temporally. In the distal region of the developing limb bud, HOXA11 and HOXA13 show different levels of expression as the limb bud grows (see Fig. S2 in the supplementary material). This may be because the amounts of HOXA11 and HOXA13 transcripts increase in each distal cell, and it is also likely that the change in expression domain contributes to the change in expression level in the distal region. As can be seen in the Fig. 6, onset of HOXA13 expression in the limb bud occurs as a small narrow domain of the posterior-distal peripheral region (see also Yokouchi et al., 1991; Nelson et al., 1996). The domain then expands anteriorly and proximally to encompass the entire autopod. In addition, the HOXA13-expressing domain does not fully cover the prospective autopod region until stage 26 (data not shown), suggesting that change in HOXA expression occurs also in the more proximal limb bud. The above observations do not support the idea of the progress zone model – that all cells within the progress zone should make their internal 'clock' active and change the clock coordinately – but they rather indicate heterogeneity in the distal region. As discussed already, however, the heterogeneity of HOXA expression is not due to mosaic distribution of HOXA11- and HOXA13-expressing cells but due to regional difference along the PD axis, suggesting that cells in different positions along the PD axis gradually acquire different properties. The sequential difference in cell affinity and graded accumulation of N-cadherin protein along the PD axis (Yajima et al., 1999; Yajima et al., 2002) also support this idea.

Overall, our results suggest that, (1) a limb bud at stage 19 has already regionalized the proximal compartments (for the stylopod and zeugopod) in terms of developmental fate as the pre-specification model proposes; (2) the early-stage limb bud does not have clear regionalization of the distal region (for the zeugopod and autopod) as the progress zone model suggests; (3) it is around stage 23 that three compartments for the stylopod, zeugopod and autopod are established in the limb bud; (4) the distal region has a mixable condition that allows cells to intermingle with each other; and (5) regional heterogeneity along the PD axis exists even in the distal region. Molecular mechanisms for each process of the PD axis formation remain to be elucidated.

We are grateful to Dr Cheryll Tickle for critical reading of this manuscript and helpful comments on it. We are also grateful to Drs Hiroyuki Ide, Hiroaki Yamamoto, and Sayuri Yonei-Tamura for many insightful discussions. This work was supported by research grants from the Ministry of Education, Science, Sports and Culture of Japan.

Supplementary material

Supplementary material for this article is available at http://dev.biologists.org/cgi/content/full/134/7/1397/DC1

References

Barna, M., Pandolfi, P. P. and Niswander, L. (2005). Gli3 and Plzf cooperate in proximal limb patterning at early stages of limb development. *Nature* **436**, 277-281.

Bowen, J., Hinchliffe, J. R., Horder, T. J. and Reeve, A. M. (1989). The fate map of the chick forelimb-bud and its bearing on hypothesized developmental control mechanisms. *Anat. Embryol.* **179**, 269-283.

Clarke, J. D. and Tickle, C. (1999). Fate maps old and new. *Nat. Cell Biol.* **1**, E103-E109.

Corson, L. B., Yamanaka, Y., Lai, K. M. and Rossant, J. (2003). Spatial and temporal patterns of ERK signaling during mouse embryogenesis. *Development* **130**, 4527-4537.

Dudley, A. T., Ros, M. A. and Tabin, C. J. (2002). A re-examination of proximodistal patterning during vertebrate limb development. *Nature* **418**, 539-544.

Eblaghie, M. C., Lunn, J. S., Dickinson, R. J., Munsterberg, A. E., Sanz-Ezquerro, J. J., Farrell, E. R., Mathers, J., Keyse, S. M., Storey, K. and Tickle, C. (2003). Negative feedback regulation of FGF signaling levels by Pyst1/MKP3 in chick embryos. *Curr. Biol.* **13**, 1009-1018.

Hamburger, V. and Hamilton, H. L. (1951). A series of normal stages in the development of the chick embryo. *Dev. Dyn.* **195**, 231-272.

Hashimoto, K., Yokouchi, Y., Yamamoto, M. and Kuroiwa, A. (1999). Distinct signaling molecules control Hoxa-11 and Hoxa-13 expression in the muscle precursor and mesenchyme of the chick limb bud. *Development* **126**, 2771-2783.

Hinchliffe, J. R. (1977). The chondrogenic pattern in chick limb morphogenesis: a problem of development and evolution. In *Vertebrate Limb and Somite Morphogenesis* (ed. D. A. Ede, J. R. Hinchliffe and M. J. Balls), pp. 293-310. Cambridge: Cambridge University Press.

Kawakami, Y., Rodriguez-Leon, J., Koth, C. M., Buscher, D., Itoh, T., Raya, A., Ng, J. K., Esteban, C. R., Takahashi, S., Henrique, D. et al. (2003). MKP3 mediates the cellular response to FGF8 signalling in the vertebrate limb. *Nat. Cell Biol.* **5**, 513-519.

Kimura, W., Yasugi, S., Stern, C. D. and Fukuda, K. (2006). Fate and plasticity of the endoderm in the early chick embryo. *Dev. Biol.* **289**, 283-295.

Lewis, J. H. (1975). Fate maps and the pattern of cell division: a calculation for the chick wing-bud. *J. Embryol. Exp. Morphol.* **33**, 419-434.

Li, S. and Muneoka, K. (1999). Cell migration and chick limb development: chemotactic action of FGF-4 and the AER. *Dev. Biol.* **211**, 335-347.

Mallein-Gerin, F., Kosher, R. A., Upholt, W. B. and Tanzer, M. L. (1988). Temporal and spatial analysis of cartilage proteoglycan core protein gene expression during limb development by in situ hybridization. *Dev. Biol.* **126**, 337-345.

Minowada, G., Jarvis, L. A., Chi, C. L., Neubuser, A., Sun, X., Hacohen, N., Krasnow, M. A. and Martin, G. R. (1999). Vertebrate Sprouty genes are induced by FGF signaling and can cause chondrodysplasia when overexpressed. *Development* **126**, 4465-4475.

Nelson, C. E., Morgan, B. A., Burke, A. C., Laufer, E., DiMambro, E., Murtaugh, L. C., Gonzales, E., Tessarollo, L., Parada, L. F. and Tabin, C. (1996). Analysis of Hox gene expression in the chick limb bud. *Development* **122**, 1449-1466.

Richardson, M. K., Jeffery, J. E. and Tabin, C. J. (2004). Proximodistal patterning of the limb: insights from evolutionary morphology. *Evol. Dev.* **6**, 1-5.

Saunders, J. W., Jr (1948). The proximo-distal sequence of origin of the parts of the chick wing and the role of the ectoderm. *J. Exp. Zool.* **282**, 628-668.

Saunders, J. W., Jr (2002). Is the progress zone model a victim of progress? *Cell* **110**, 541-543.

Stark, R. J. and Searls, R. L. (1973). A description of chick wing bud development and a model of limb morphogenesis. *Dev. Biol.* **33**, 138-153.

Stocum, D. L. (1975). Outgrowth and pattern formation during limb ontogeny and regeneration. *Differentiation* **3**, 167-182.

Summerbell, D. (1974). A quantitative analysis of the effect of excision of the AER from the chick limb-bud. *J. Embryol. Exp. Morphol.* **32**, 651-660.

Summerbell, D. (1976). A descriptive study of the rate of elongation and differentiation of the skeleton of the developing chick wing. *J. Embryol. Exp. Morphol.* **35**, 241-260.

Summerbell, D. and Lewis, J. H. (1975). Time, place and positional value in the chick limb-bud. *J. Embryol. Exp. Morphol.* **33**, 621-643.

Sun, X., Mariani, F. V. and Martin, G. R. (2002). Functions of FGF signalling from the apical ectodermal ridge in limb development. *Nature* **418**, 501-508.

Suzuki, M. and Kuroiwa, A. (2002). Transition of Hox expression during limb cartilage development. *Mech. Dev.* **118**, 241-245.

Tickle, C. and Wolpert, L. (2002). The progress zone – alive or dead? *Nat. Cell Biol.* **4**, E216-E217.

Vargesson, N., Clarke, J. D., Vincent, K., Coles, C., Wolpert, L. and Tickle, C. (1997). Cell fate in the chick limb bud and relationship to gene expression. *Development* **124**, 1909-1918.

Wolpert, L. (1969). Positional information and the spatial pattern of cellular differentiation. *J. Theor. Biol.* **25**, 1-47.

Wolpert, L. (2002). Limb patterning: reports of model's death exaggerated. *Curr. Biol.* **12**, R628-R630.
Wolpert, L., Lewis, J. and Summerbell, D. (1975). Morphogenesis of the vertebrate limb. *Ciba Found. Symp.* **0**, 95-130.
Yajima, H., Yoneitamura, S., Watanabe, N., Tamura, K. and Ide, H. (1999). Role of N-cadherin in the sorting-out of mesenchymal cells and in the positional identity along the proximodistal axis of the chick limb bud. *Dev. Dyn.* **216**, 274-284.
Yajima, H., Hara, K., Ide, H. and Tamura, K. (2002). Cell adhesiveness and affinity for limb pattern formation. *Int. J. Dev. Biol.* **46**, 897-904.
Yamamoto, M., Gotoh, Y., Tamura, K., Tanaka, M., Kawakami, A., Ide, H. and Kuroiwa, A. (1998). Coordinated expression of Hoxa-11 and Hoxa-13 during limb muscle patterning. *Development* **125**, 1325-1335.
Yokouchi, Y., Sasaki, H. and Kuroiwa, A. (1991). Homeobox gene expression correlated with the bifurcation process of limb cartilage development. *Nature* **353**, 443-445.
Yonei, S., Tamura, K., Ohsugi, K. and Ide, H. (1995). MRC-5 cells induce the AER prior to the duplicated pattern formation in chick limb bud. *Dev. Biol.* **170**, 542-552.